5-2021

Ball-on-Ring Test Validation for Equibiaxial Flexural Strength Testing of Engineered Ceramics

Adrianna E. Lupercio
Boise State University

Ehsan Moshkelgosha
Boise State University

Riley C. Winters
Boise State University

Cayden Doyle
Boise State University

Mahmood Mamivand
Boise State University

See next page for additional authors

Received: 10 December 2020 | Revised: 1 March 2021 | Accepted: 9 March 2021

DOI: 10.1002/ces2.10085

ORIGINAL ARTICLE

International Journal of Ceramic Engineering & Science

Ball-on-ring test validation for equibiaxial flexural strength testing of engineered ceramics

Adrianna E. Lupercio[1,2] | **Ehsan Moshkelgosha**[1,3] | **Riley C. Winters**[1,2] | **Cayden Doyle**[1,2] | **Mahmood Mamivand**[3] | **Andrew T. Nelson**[4] | **Brian J. Jaques**[1,2]

[1]Boise State University, Micron School of Materials Science and Engineering, Boise, ID, USA

[2]Center for Advanced Energy Studies, Idaho Falls, ID, USA

[3]Mechanical and Biomedical Engineering, Boise State University, Boise, ID, USA

[4]Oak Ridge National Laboratory, Oak Ridge, TN, USA

Correspondence
Brian J. Jaques, Boise State University, Micron School of Materials Science and Engineering, Boise, ID.
Email: BrianJaques@boisestate.edu

Funding information
UT-Battelle, LLC, Grant/Award Number: DE-AC05-00OR22725; Integrated University Program, Grant/Award Number: DOE-FOA-0001487

Abstract

The validation of a ball-on-ring, equibiaxial flexural strength method to obtain the transverse rupture strength (TRS) of right cylindrical ceramic specimens was performed in this study. Validation of the test method was achieved using commercially available engineered high purity alumina disks and finite element (FE) model analysis. The validated fixture was then used to obtain the TRS and Weibull statistical analysis of MgO-partially stabilized zirconia (MSZ) and Y_2O_3-partially stabilized zirconia (YSZ) ceramic disks. TRS data for alumina, MSZ, and YSZ agreed with the TRS values reported in the literature. A statistically relevant number of samples ($N > 30$) for each material were tested to allow for a Weibull statistical analysis. Weibull parameters for these materials were within the expected values for engineered ceramics. The characteristic strength for alumina, MSZ, and YSZ were determined to be 289, 786, and 814 MPa, respectively. The Weibull modulus was determined between 10 and 25 for each material, which is typical of engineered ceramics. In addition, FE model results were in close agreement with experimental fracture values for the three ceramic materials tested in this study.

KEYWORDS

alumina, zirconia: partially stabilized, Weibull statistics, finite element analysis, rupture

1 | INTRODUCTION

Due to the brittle nature of ceramics, their mechanical properties are rarely measured using typical tensile tests employed for metals. Historically, the flexural strength, or the transverse rupture strength (TRS), of ceramics has been commonly determined using 3- and 4-point bend tests which uses $3 \times 4 \times 45$ mm rectangular bend bars per ASTM standard C1161-13.[1] However, it is difficult to perform a comprehensive statistical analysis of TRS data using bend bar techniques due to difficulties in producing samples with the required geometries and dimensions using traditional powder metallurgy techniques. In addition, extraneous flaws introduced along the edges during the fabrication of the bend bars often become the origin of fracture.[2] In contrast, the equibiaxial flexural strength test also referred to as a TRS test, requires a simple right cylindrical test specimen. Additionally, 3- and 4-point bend tests only provide information about the mechanical properties of ceramic materials under uniaxial loading.[2] It is important to use other methods to evaluate the mechanical properties under multiaxial loading states to obtain a more accurate rupture strength, particularly for specimens loaded

in nonuniaxial states during service. Unlike 3- and 4-point flexural strength tests, TRS tests measure mechanical properties in a biaxial stress state, which can better predict the behavior of ceramic parts during operation.[2]

The TRS test offers significant advantages over the bend bar techniques, namely, fabrication costs and time can be significantly reduced, and extraneous flaws can be avoided due to the lack of required machining of TRS test specimens. The simple right cylindrical geometry allows for rapid fabrication of test specimens used to obtain the sample size ($N > 30$) required to develop a statistically relevant description of the mechanical behavior of ceramic materials ($N < 30$ does not allow a distinction between Weibull, Gaussian or other similar distribution functions).[3] Additionally, the TRS test method provides reduced friction during testing and the quality of the edges does not influence the measurement.[2] Two disadvantages of this test method are the reduced volume being tested and the assumptions used to calculate the contact radius between the test sample and the loading ball as determined by the sample thickness and loading ball radius. The advantages of TRS tests seem to outweigh the disadvantages, and while some of the flexure data are available, several common ceramic materials are lacking, specifically for the ball-on-ring method. Furthermore, in the literature, few studies using bend bar techniques or biaxial tests have completed the necessary sample tests for the rigorous statistics needed to obtain Weibull parameters. This study focuses on the qualification of a ball-on-ring TRS test fixture for obtaining rupture strength data using alumina as a benchmark material and comparing results with a finite element (FE) model. The ball-on-ring TRS test fixture can then be used to obtain fracture strength data for magnesia stabilized zirconia (MSZ) and yttria stabilized zirconia (YSZ) to generate a statistically relevant volume of fracture data to perform a Weibull statistical analysis.

2 | TESTING THEORY

2.1 | Equibiaxial flexural test

Common equibiaxial flexural strength tests include ring-on-ring, piston-on-3-balls or the ball-on-ring methods, all of which work to reduce friction during testing.[4] Several studies [3-5] have used Equation 1 to calculate the transverse stress (σ) and obtain the TRS of ceramics:

$$\sigma = \frac{A \times F}{t^2} \tag{1}$$

where t is the specimen thickness, F is the applied force, and A is a dimensionless factor that depends on the geometry of the specimen and loading ball, the ring diameter, and the Poisson's ratio of the loading ball and test materials. The factor A is calculated using Equation 2 for a ball-on-3 balls or ball-on-ring test:

$$A = \frac{3}{4 \times \pi}\left[\left(2(1+v_s) \times \ln\frac{a}{b}\right) + \frac{(1-v_s)(2a^2-b^2)}{2R^2} + (1+v_s)\right] \tag{2}$$

where v_S is the Poisson's ratio of the test material, a is the radius of the support ring, R is the radius of the test specimen, and b is the contact radius of the loading ball. The contact radius of the loading ball b can be calculated using an equivalent radius through Equation 3:

$$\overline{b} = \sqrt{1.6b^2 + t^2} - 0.675t \tag{3}$$

which can be reduced to $-\overline{b} = \frac{t}{3}$.[5-7]

2.2 | Weibull statistics theory

The fracture of brittle materials does not follow the same trend as metallic materials. Instead, cracks typically initiate from flaws in the material and the strength of the materials is dependent on the size of the largest critical flaw in each specimen.[3] The statistical behavior of brittle materials indicates that the probability of failure increases with increasing load and with larger sample volumes.[8] The fracture analysis of these types of materials requires understanding the behavior of many cracks which are assumed to be stochastically distributed in the material. The TRS of a brittle ceramic material cannot be described using a single stress value. Hence, a probability function must be used to quantify the characteristic strength and probability of failure or reliability. One common method of analyzing the statistical fracture of ceramics is the Weibull distribution of the probability of failure. Describing fracture behavior using Weibull statistics assumes that (a) the structure must fail if one single flaw becomes critical and (b) large flaws do not interact.[8]

The classical relationship for the probability of failure (P_f) using two parameter Weibull statistics is shown in Equation 4:

$$\ln\ln\left(\frac{1}{1-P_f}\right) = m \times \ln\left[\frac{\sigma_f}{\sigma_0}\right] \tag{4}$$

where σ_f is the fracture strength, σ_0 is the characteristic strength, and m is the Weibull modulus. The Weibull parameters σ_0 and m can then be determined by plotting the equation in the form of a line, $y = m \times x + b$.[9] The characteristic strength is defined as the stress value at which 63.2% of all samples fail and the Weibull modulus provides information about fracture data scatter of the samples.[10] The larger the Weibull modulus the less

variation in fracture stress and the higher the degree of homogeneity between samples. However, if fracture data does not follow a straight line, the classical two parameter Weibull distribution does not accurately characterize sample reliability.[11] In this case, it is best to analyze the data set using a curve fitting software to determine the most appropriate statistical distribution (ie, mixed, Weibull, three parameter Weibull, Gaussian, exponential, etc.).

3 | EXPERIMENTAL PROCEDURE

3.1 | Specimen preparation

Commercially purchased ceramic materials of 99.8% pure alumina (CoorsTek Inc.), 3 mol% Y_2O_3-partially stabilized zirconia (YSZ) (Ortech Inc.), and MgO-partially stabilized zirconia (MSZ) (Ortech Inc.), were purchased in the form of right cylindrical rods with a diameter of 15.9 mm. From these rods, test specimens were cut close to 1.5 mm in height (Figure 1) using a low-speed saw with a low concentration diamond blade and a propylene glycol cutting fluid. The flat faces of the specimens were ground parallel to approximately 1.5 mm in height using an UltraPrep 45 μm diamond disc (Buehler) and then fine-tuned to 1.5 ± 0.02 mm in height using 180 grit silicon carbide paper (Figure 1). This method allowed for greater control of the sample preparation as the diamond discs ground through the material at a faster rate than the 180 grit silicon carbide paper. Sample height was measured using a micrometer with five perimeter and three center measurements, which were averaged to produce the height value used in the TRS calculations.

3.2 | Specimen characterization

Samples were characterized using several methods, including X-ray diffraction (XRD) (Rigaku Miniflex, 600) to obtain the phase of the material, nondispersive infrared (NDIR) spectroscopy using an oxygen analysis instrument (LECO, ON836), and scanning electron microscopy (SEM) (Hitachi, S-3400N) to obtain microstructure and fracture surface images in addition to a chemical analysis using energy dispersive X-ray spectroscopy (EDS).

Samples were pulverized using a percussion mill and doped with a small amount of a silicon standard (NIST SRM 640d) prior to performing powder XRD. Un-doped powder of each sample type was weighed out and combusted in a nickel capsule and graphite crucible to obtain the amount of oxygen in each material using NDIR spectroscopy. Each sample type was polished to 0.5 μm and a thermal etch was performed to obtain grain boundary relief for grain size and a chemical analysis using SEM and EDS. Thermally etched samples and fracture surfaces of tested samples were carbon coated prior to imaging and chemical analysis.

3.3 | Transverse rupture strength tests

This study uses a ball-on-ring TRS test fixture as shown in Figure 2. The fixture consists of a base with a ring diameter of 13 mm, set screws to center the sample, a punch with an imbedded loading ball, and a punch alignment sleeve. The imbedded loading ball is made of tungsten carbide while the rest of the fixture is made of a high strength CPM 10V tool steel.

The applied load was generated using an 810 series materials test system (MTS) mechanical test frame. The MTS TestSuite software recorded the applied load and the displacement at a rate of 4 Hz. The generated force data are used to calculate transverse stress using Equations 1 and 2 above. The maximum calculated stress values were recorded as the TRS for each sample.

3.4 | Finite element analysis

Numerical simulations were performed using the COMSOL Multiphysics software with an implicit static method. All interacting elements in this simulation were produced in COMSOL and chosen as deformable bodies. A two-dimensional axisymmetric model was generated by assuming a linear isotropic elasticity, described through Hooke's generalized law, and considering the geometrical axisymmetry of the test apparatus, material properties, and loading conditions. Making these simplifications enables a greater mesh control and higher accuracy while reducing computational costs and time. Figure 3 represents the geometry of the axisymmetric model used in this study. Table 1 summarizes the material

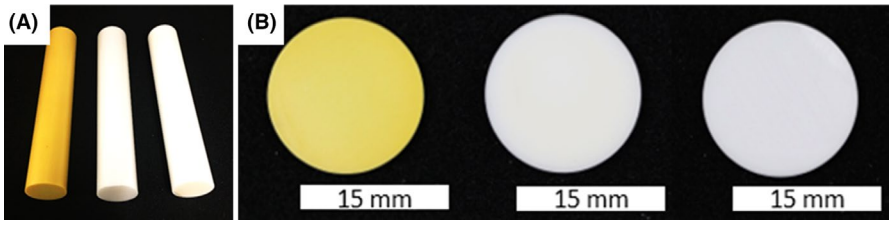

FIGURE 1 Macro images of A, commercially purchased ceramic rods and B, the faces of the specimens after preparation for TRS testing in order from left to right: MSZ, alumina, and YSZ

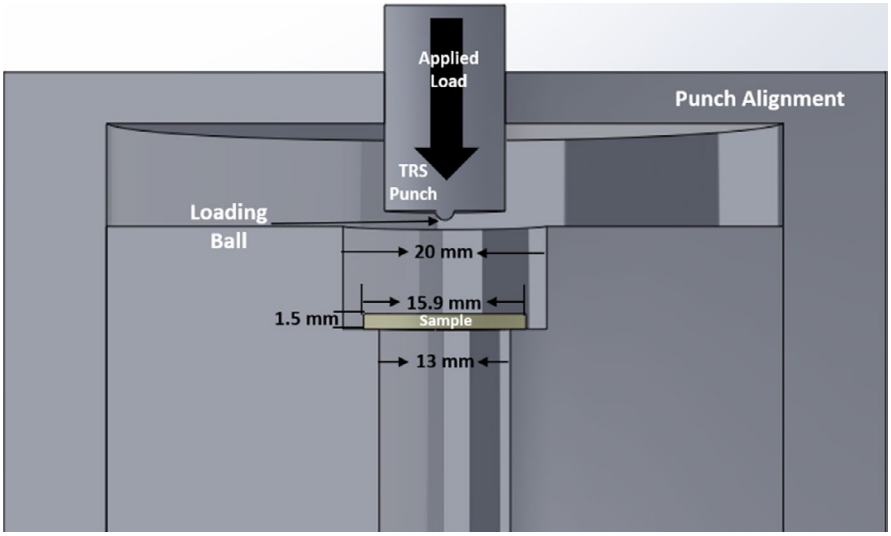

FIGURE 2 Cross section schematic of the ball-on-ring TRS test fixture for right cylindrical samples

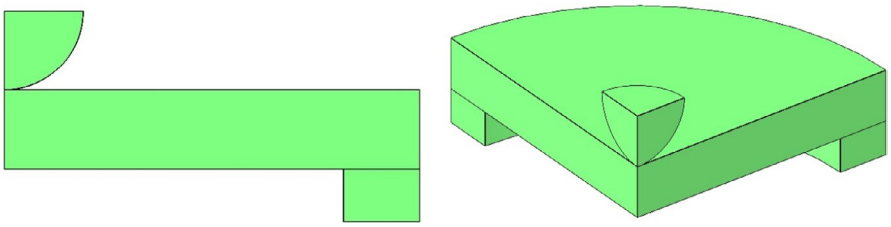

FIGURE 3 FE model geometry of the TRS test with the axisymmetric simplification

TABLE 1 Material property parameters used in FE model

Loading Ball[12]	Material Properties	YSZ[13-17]	Material Properties
The radius of the loading ball	1.5 mm	Density	6.08 g/cm^3
Density	15.7 g/cm^3	Archimedes density (measured)	5.99 g/cm^3
Elastic modulus	600 GPa	Elastic modulus	210 GPa
Poisson's ratio	0.22	Poisson's ratio	0.23
Alumina[18,19]		**MSZ[20]**	
Density	3.92 g/cm^3	Density	5.72 g/cm^3
Archimedes density (measured)	3.90 g/cm^3	Archimedes density (measured)	5.74 g/cm^3
Elastic modulus	370 GPa	Elastic modulus	200 GPa
Poisson's ratio	0.22	Poisson's ratio	0.23

properties of the test specimens and loading ball that are used as input parameters in the FE model to evaluate the TRS fixture and are also used in the experimental calculations.

Ceramic samples, supporting fixture, and the ball-loading sphere were considered as isotropic linear elastic materials defined by the Hooke's generalized elasticity law. The contact between the loading ball, the sample, and the support ring was specified via a surface-to-surface discretization system considering frictionless conditions. This assumes a tangential response and a penalty method as a constraint enforcement method for the normal behavior. The support ring was fixed, while the loading ball was constrained to move only in the z-direction to elicit a response between the contacting elements of the ball-on-ring test.[21] A rectangular mesh of 0.1 mm for the loading-ball and support-ring were used, while a mapped mesh of 0.04 mm was used for the sample, which yields 8220 elements and 48 730 degrees of freedom. Finally, the FE model used the experimental load at fracture, which is used in Equations 1 and 2 for determining TRS, to calculate the TRS for samples of each material.

4 | RESULTS

4.1 | Specimen characterization

4.1.1 | Chemical analysis

The compositions of the samples were analyzed using EDS and NDIR spectroscopy. NDIR was used to determine the concentration of oxygen, in wt%, of each sample type. EDS was used to determine if any major impurities were present in each sample (ie, Mg, Zr, Al, etc.). Accordingly, EDS did not detect any impurities in the alumina, although a small amount of hafnium (0.4-0.5 at %) was detected in both the

TABLE 2 NDIR and EDS results verify sample composition for alumina, MSZ, and YSZ. Small amounts of hafnium (0.4-0.5 at %) were detected in the MSZ and YSZ samples

NDIR		EDS		
Material	**O at%**	**Element at%**	**Element at%**	**Composition**
Alumina	52 ± 4.3	38 ± 1.6 (Al)	–	Al_2O_3
MSZ	67 ± 0.3	30 ± 2.0 (Zr)	3.4 ± 0.6 (Mg)	10 mol% MgO-ZrO_2
YSZ	69 ± 2.2	30 ± 0.5 (Zr)	1.4 ± 0.5 (Y)	2.5 mol% Y_2O_3-ZrO_2

Note: Relative error is presented as a standard deviation from the average value.

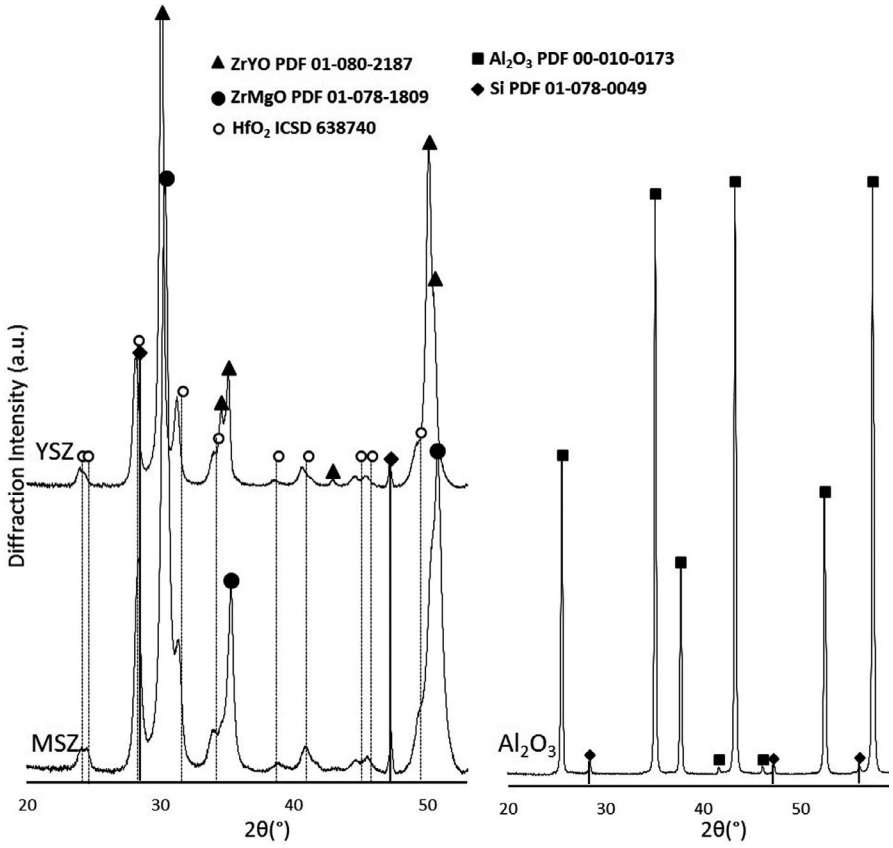

FIGURE 4 Powder XRD patterns for alumina, MSZ, and YSZ confirm the phase of the test specimens and shows small amounts of HfO2 in the MSZ and YSZ samples. EDS chemical analysis detected the presence of hafnium for the MSZ and YSZ samples

MSZ and YSZ. For each sample, the mass fraction of each element (determined using EDS) and the mass fraction of oxygen (determined using NDIR spectroscopy) were converted to the atomic percent of each constituent element assuming stoichiometric concentrations of zirconia, as shown in Table 2. Sample analysis indicates there is <2 wt% excess oxygen in the MSZ and YSZ samples. Finally, sample phases were verified using powder XRD, as shown in Figure 4. An HfO_2 phase was observed in both the MSZ and YSZ samples.

4.1.2 | Microstructural analysis

Scanning electron microscopy was used to obtain images of the alumina, MSZ, and YSZ microstructure to measure average grain size, as shown in Figure 5. Archimedes and geometric density measurements for these materials were recorded in Table 3. Grain size measurements were performed on thermally etched samples using ASTM standard E112-13 for alumina and ASTM standard E112-12 for MSZ and YSZ; grain size measurements are also recorded in Table 3.

4.2 | Transverse rupture strength tests

The TRS values found in this study, using the ball-on-ring fixture, agree with those found in literature for MSZ and YSZ, as shown in Table 4. The lower end TRS values for alumina are about 36 MPa below the range found in the literature search performed. The TRS values in the literature, reported in Table 4, were obtained using the 3-point bend and piston-on-3 balls TRS test methods. Most of the studies did not report specific material characteristics (ie, density, microstructure, etc.). TRS values can span a wide range, depending on the density, microstructure, composition, sample preparation, and flaw size distribution. The characteristic strength

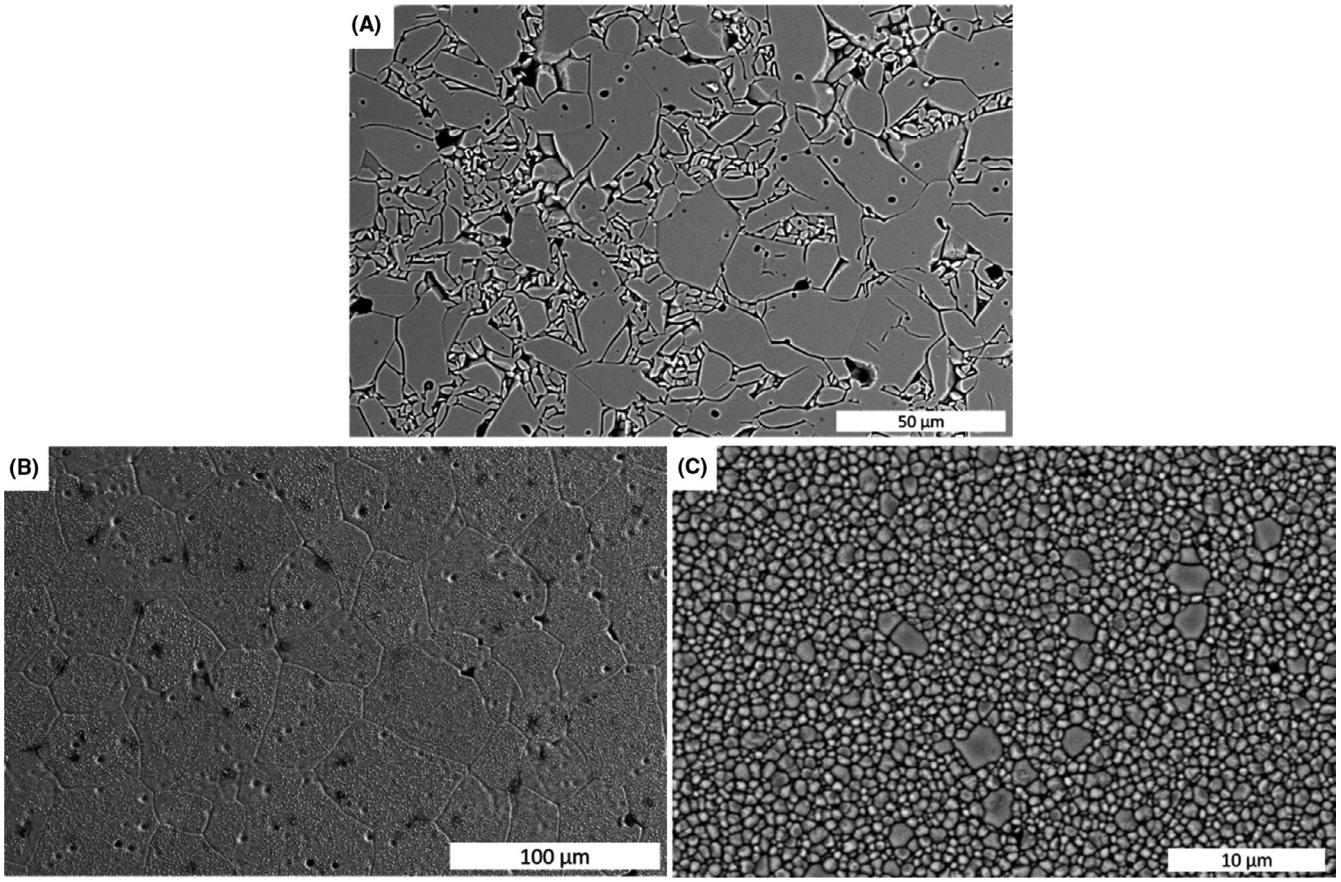

FIGURE 5 SEM micrographs of microstructure for thermally etched A, alumina, B, MSZ, and C, YSZ test specimens. Specimens have a grain size of 5.6-63.5 µm (trimodal), 35 µm, and 0.7-1.9 µm (bimodal), respectively

TABLE 3 Density and grain size measurements for alumina, MSZ, and YSZ

Material	Density			Grain Size (µm)	Grain Size Mode
	Reference (g/cm^3)	Archimedes (±2% TD)	Geometric (±2%TD)		
Alumina	3.92[18]	99	97	5.6, 11.2, 63.5	trimodal
MSZ	5.75[20]	99	97	35	unimodal
YSZ	6.08[17]	98	94	0.7, 1.9	bimodal

TABLE 4 TRS values found in the literature (using 3-point bend and piston-on-3 balls tests) and determined in this study for alumina, MSZ, and YSZ

Material	TRS Reported in Literature (MPa)	Reference	TRS Range Determined through This Study (MPa)
Alumina	266-550	[10,18,22,23]	230-328
MSZ	400-900	[24-27]	611-893
YSZ	320-1240	[28-31]	595-936

for the alumina samples is within the TRS range reported in the literature while the lowest recorded TRS value is slightly below the reported TRS range. Figure 6 shows macro images of typical fractured samples for MSZ, alumina, and YSZ. The samples fractured into two to five pieces, with the majority (>75%) of them breaking into three to four pieces. Figure 7 shows a representative stress vs displacement curve for alumina, MSZ, and YSZ.

4.3 | Fractography

Figure 8 shows SEM images of the fracture surface for alumina, MSZ, and YSZ that give some indication of the fracture mode for each sample type. The alumina samples have a trimodal microstructure that appears to impact the fracture mode. In the MSZ samples, transgranular failure was observed in the SEM images. High-magnification images of YSZ reveal an intergranular fracture mode.

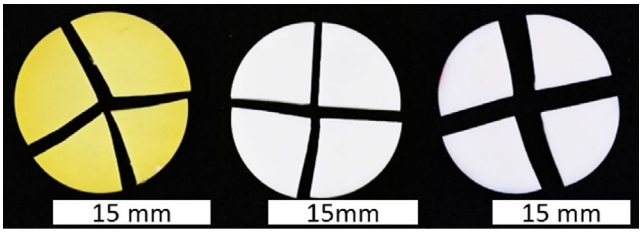

FIGURE 6 Samples post TRS tests from left to right MSZ, alumina, and YSZ

4.4 | Statistical analysis

Weibull statistics were used to evaluate the characteristic strength and Weibull modulus of all three ceramic specimen types using the Reliasoft Weibull^{++} software[32] to plot and curve fit the data. Weibull parameters for alumina and MSZ were calculated using a two parameter Weibull function and fit with a straight line where the slope of the line is taken as the Weibull modulus. The characteristic strength is extracted

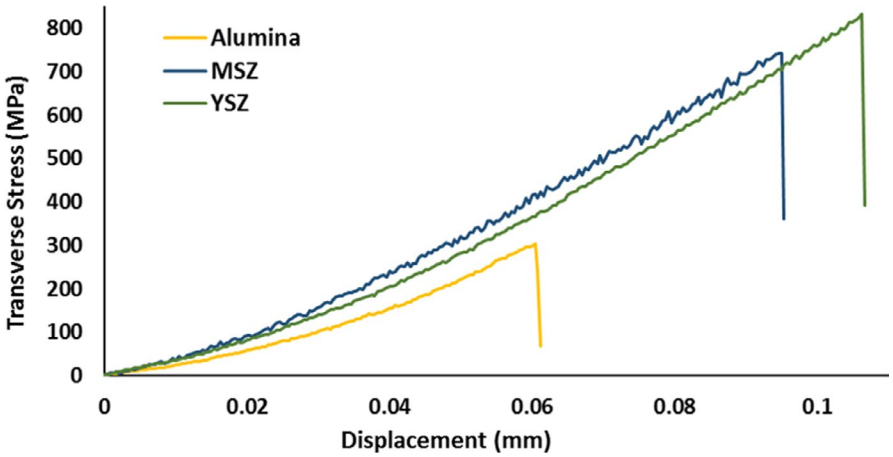

FIGURE 7 Representative stress vs displacement curves for each specimen type

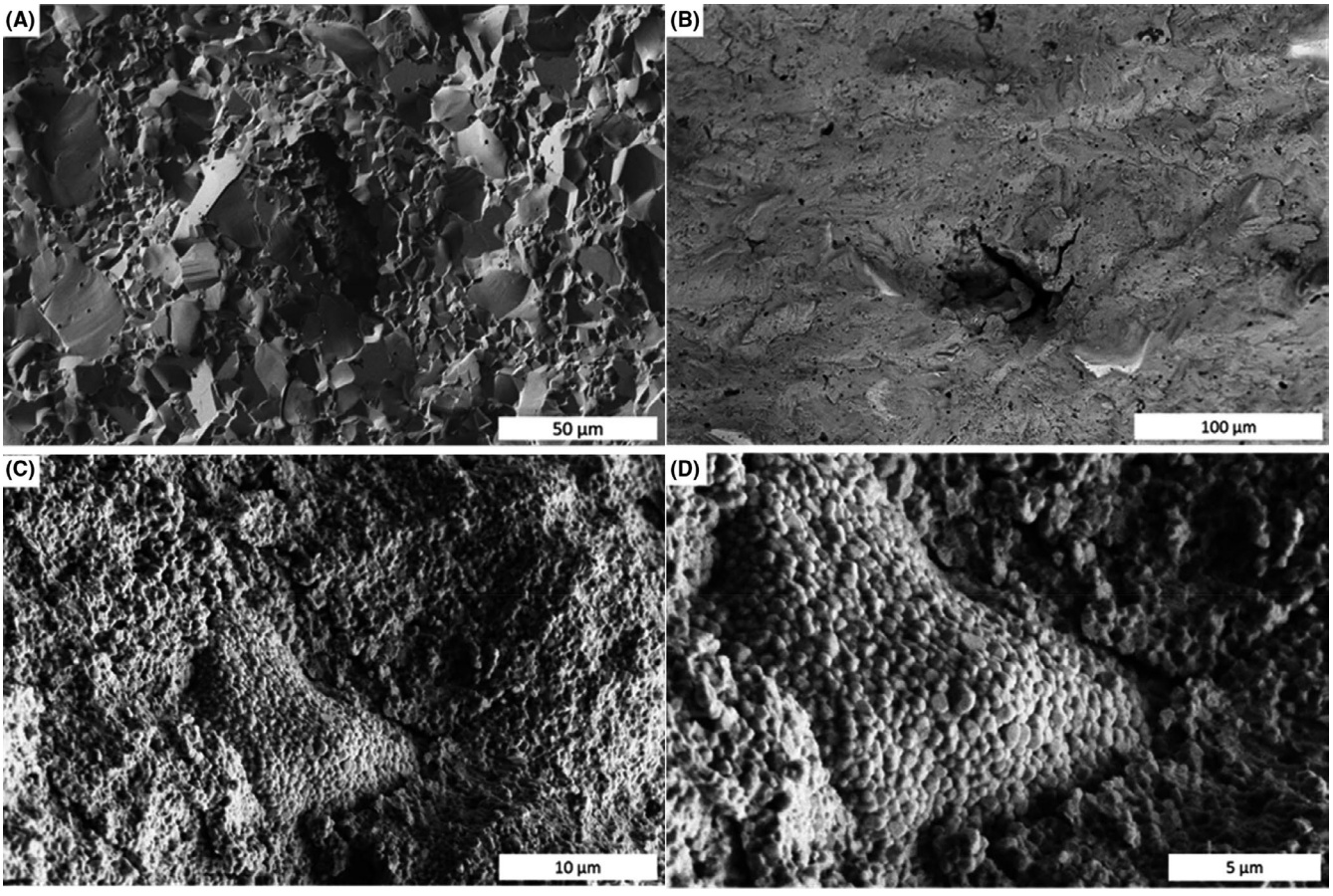

FIGURE 8 SEM fracture images of TRS tested samples from left to right A, alumina, B, MSZ, C and D YSZ

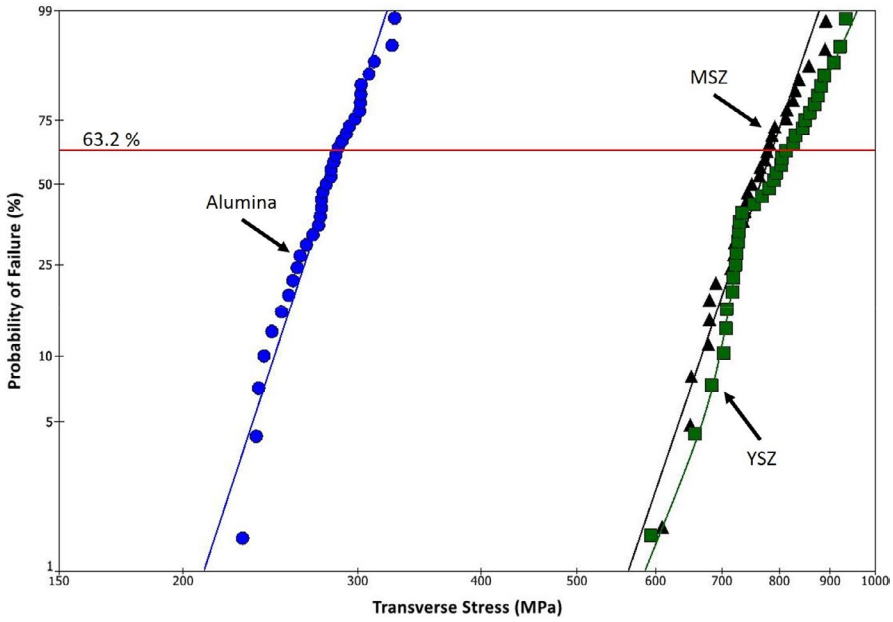

FIGURE 9 The characteristic strength and Weibull modulus for alumina and MSZ were 289 and 786 MPa and 14.3 and 13.8, respectively. A mixed Weibull statistics plot determined the overall characteristic strength and Weibull modulus for YSZ at 814 MPa and 22.2

TABLE 5 Weibull parameters for the alumina, MSZ, and YSZ samples

Material	Average TRS (MPa)	Portion of Population (%)	Characteristic Strength [σ_0] (MPa)	Weibull Modulus [m]	Regression Fit [ρ]	No. Test Samples
Alumina	279	–	289	14.3	0.98	35
MSZ	757	–	786	13.8	0.98	33
YSZ subpopulation 1	785	27.5	729	50.0	0.99	34
YSZ subpopulation 2		72.5	846	11.6		
YSZ overall data set		–	814	22.2		

where the probability of failure (P_f) is equal to 63.2%, which was found as 289 and 786 MPa for alumina and MSZ, respectively, as shown in Figure 9. The YSZ data set was fit as a mixed Weibull plot with a two subpopulation, where the slope of each line is taken as the Weibull modulus for each subpopulation. The overall characteristic strength of YSZ was calculated as 814 MPa by taking the weighted average of the characteristic strengths for each subpopulation. Table 5 lists the alumina, MSZ, and YSZ Weibull parameters, the average TRS for each sample type, and the proportion of each Weibull parameter for YSZ.

4.5 | Finite element modeling results

From experimental results for alumina, the average force registered at fracture was 340 N for a 1.50 mm sample and this value was used to calculate the uniform pressure over the loading-ball top surface area. From the simulation, it was determined that the maximum tensile biaxial stress occurs on the bottom of the disk indicated by the red area in Figure 10, with a value of 290 MPa. The experimental TRS for this sample was measured as 293 MPa which is in good agreement with the FE model results.

The predicted stress values at the tensile surface along with the radial (σ_r) and tangential (σ_t) directions, represented in Figure 11, explain how these stresses change as a function of the radial length. σ_r and σ_t are equal at the center of the tensile surface of the disk. As the radial distance increases, the difference between these two stresses also increases.[33,34] In addition, a sharp decrease in the stress pattern on the tensile surface of the specimen is clearly indicated in the plot produced by the FE model. This is due to compressive stresses where the sample makes contact along the supporting ring and indicates that it will not be a failure point in the ball-on-ring test.[21] The FE analysis was conducted for alumina, YSZ, and MSZ, and the results are given in Table 6.

5 | DISCUSSION

The TRS and Weibull parameters found in this study are close to values published in the literature using various flexural strength test methods (ie, 3-point bending and piston-on-3

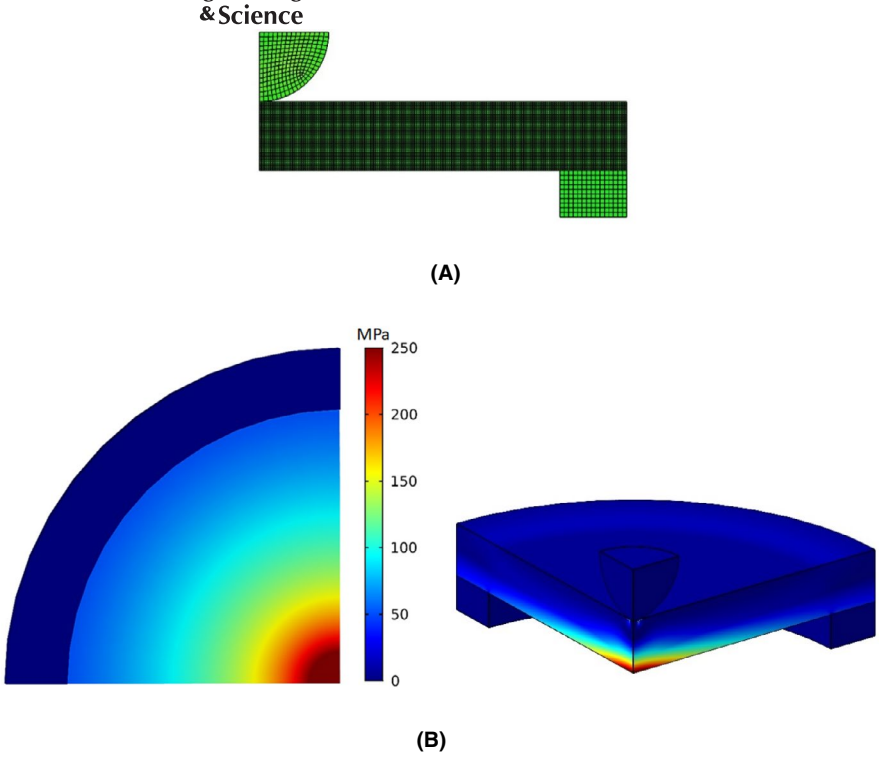

FIGURE 10 A, Mesh distribution and B, maximum-principal stress distribution on the sample

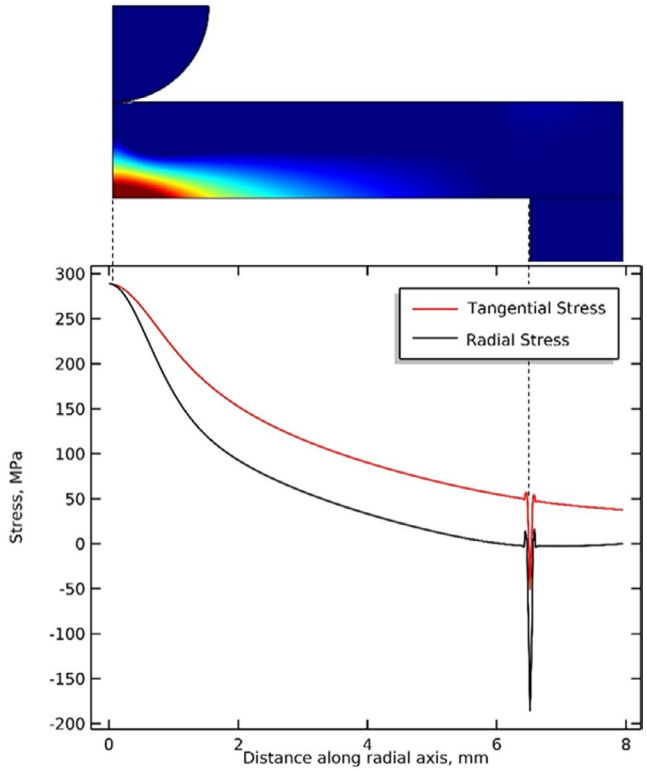

FIGURE 11 Tangential (σt) and radial (σr) stress distribution at the bottom tensile surface of the sample disk, shown in the upper portion of the figure

balls). The ball-on-ring method used in this study uses simple right cylindrical specimens, which allows for the rapid fabrication and testing of ceramic samples to perform a statistical

TABLE 6 FE modeling results and corresponding TRS values for alumina, MSZ, and YSZ samples with varying sample thickness

Material	Thickness (mm)	Load at Fracture (N)	Corresponding Experimental TRS (MPa)	FE Model TRS (MPa)
Alumina	1.50	340	293	289
	1.51	334	279	277
	1.48	309	267	279
YSZ	1.49	927	796	816
	1.51	1,061	890	881
	1.49	1,006	876	885
MSZ	1.51	995	839	824
	1.49	895	779	774
	1.50	1,050	891	894

analysis. In addition, this test method is less impacted by edge defects, which can play a significant role in fracture data obtained from bend bar samples. The ball-on-ring TRS test has several advantages over bend bar techniques; however, it is important to acknowledge sources of error and gaps in the ability to directly compare test data with the literature. Accordingly, compliance in the test fixture and mechanical test frame, surface and bulk defects introduced during sample preparation, and precise sample thickness measurements can all introduce sources of error. In addition, the majority of TRS tests performed in the literature do not address many of the factors that contribute to TRS, which makes a direct comparison difficult, including microstructure, density, imperfections, and flaw size distributions.

Alumina samples have been more extensively tested using bend bar techniques and the piston-on-3 balls test method. Hence, relative to the partially stabilized zirconia samples, more data are available on TRS values for alumina samples. Alumina was used to investigate the validity of the ball-on-ring TRS fixture in the study. Ball-on-ring TRS tests for alumina samples recorded a TRS as low as 36 MPa below the lower end of TRS values found in the literature. Given the possible sample variances (microstructure, density, etc.) from those in the literature, it is reasonable to expect some level of discrepancy. The characteristic strength is within 10% of the strength reported using Weibull statistics of 3-point bend bar tests of alumina, as published by L. Curkovic et al.[10] In addition, the FE model also validated experimental results, with its TRS calculation being within 5% of the experimental characteristic strength (Table 6). Furthermore, microstructure, flaw size distributions, and other imperfections were not directly input into the FE model as it intrinsically considers those characteristics by using the experimental fracture load.

Ball-on-ring TRS tests of MSZ and YSZ resulted in TRS values within those found in the literature. The TRS values found in literature for MSZ and YSZ have a much wider span than that of Al_2O_3. In addition to microstructure, this can be partly attributed to differences in the concentration of Y_2O_3 or MgO and impurities which can heavily impact the TRS of ceramic materials. For example, according to several numerical studies on the effects of phase transitions in zirconia where the transition leads to volume expansion, the material can undergo transformation toughening which alters the sample strength.[35-37] Using chemical analysis (ie, XRD, EDS, and NDIR) the additive concentrations of both partially stabilized zirconia samples, MSZ and YSZ (10 mol% MgO and 2.5 mol% of Y_2O_3, respectively), were determined, as shown in Table 2.

The Weibull statistics analysis for alumina, MSZ, and YSZ provided Weibull parameters that agree with values found in the literature for engineered ceramics (Table 5). The characteristic strengths were recorded as 289 MPa and 786 MPa, for alumina and MSZ, respectively, while the characteristic strength for the overall YSZ data set was determined to be 814 MPa. A typical Weibull modulus for engineered ceramics, such as the materials tested in this work, typically ranges from 10 to 20 or higher.[8] The Weibull moduli for alumina and MSZ were determined as 14.3 and 13.8, respectively, and the Weibull parameter for the overall YSZ data set was calculated as 22.2. The shape and linear fit of the Weibull curve for alumina and MSZ (Figure 9) indicates it can be well described by the two parameter Weibull distribution with the required number of samples tested, suggesting that this model is an appropriate evaluation tool for these samples. The plotted YSZ data set resulted in a slight knee shape which appeared as though it could be described by two separate Weibull curves (Figure 9). This indicated that that the data set was likely a mixed Weibull distribution with two distinct subpopulations.[38-40] This was confirmed using a Weibull curve fitting software.[32] From other studies, one possible explanation for this two failure mode is the influence of volume versus surface flaws.[41] However, to fully confirm this hypothesis, a fracture analysis would need to be performed on each tested sample to identify the fracture origin.

Overall, the fracture data for the alumina and MSZ plotted using the classical two parameter Weibull distribution and the YSZ data plotted using a mixed Weibull distribution had a regression fit (ρ) of approximately 0.98, 0.98, and 0.99, respectively. For these samples, a Weibull modulus was determined for each of the ceramics of 10-25 and the characteristic strengths (σ_0) were in good agreement with literature; which are good indications that the TRS test setup provides reliable data for these types of materials. FE modeling results also validate the MSZ and YSZ characteristic strength results with an average difference of <8% difference (Table 6).

In the limited number of samples examined, fracture due to edge defects was not observed but there is also not enough evidence to make any claims on where fractures originated. In this study, it was determined that alumina had a mixture of intergranular and transgranular fractures, which is commonly noted in high-density alumina.[42] The mixture of intergranular and transgranular fractures appears to coincide with the trimodal microstructure observed in the alumina samples. From the SEM image Figure 8A, we found that the larger grains appear to fracture transgranularly while the smallest grains fracture intergranularly. The MSZ samples appeared to exhibit a transgranular fracture mode, while YSZ samples have an intergranular fracture mode, as shown in SEM images B and C from Figure 8. In a report by Rice et al.,[43] it was noted that intergranular fracture is dominant in fine grained samples, and although this fracture mode is typically associated with lower strength samples, it is also associated with a fine microstructure, which at lower temperatures means higher strengths. The characteristic strengths for the MSZ and YSZ samples are in line with fracture surface images where YSZ, with a finer microstructure, resulted in a higher TRS.

In summary, the above discussion ties together the experimental and modeling results which indicate that the ball-on-ring TRS test fixture provides reliable TRS data. Reduced difficulty in sample fabrication for the test method increases the feasibility of obtaining test data of samples with varying characteristics (ie, microstructure, chemistry, etc.) in shorter time frames. Finally, due to the ease of sample fabrication larger sample sets can be tested to obtain a statistically relevant analysis.

6 | CONCLUSIONS

This study validates a ball-on-ring TRS test method using high purity alumina to obtain TRS and Weibull parameters.

In addition, a finite element model was used to validate experimental TRS results. The ball-on-ring TRS fixture was then used to obtain the TRS and Weibull parameters of MSZ and YSZ. FE modeling was used to further validate experimental results for both phases of the partially stabilized zirconia. Experimental TRS values and characteristic strengths generally agreed with the values found in the literature for each respective material. For all three material types, the Weibull modulus was determined to be between 10 and 25, which is a typical range for engineered ceramics. The fracture data for alumina and MSZ fit the two parameter Weibull distribution well. Although the YSZ fracture data required a mixed Weibull distribution with a two subpopulation, the resulting analysis had a good regression fit. The agreement between calculated Weibull parameters and the literature, along with well fit data, implies this type of statistical analysis is an appropriate evaluation method for these data sets. Experimental data suggests that the ball-on-ring, TRS test method used in this study is a valid method to obtain the TRS of engineered ceramics.

Experimental TRS values, obtained from the ball-on-ring TRS fixture, were also compared with the model developed using the FE method. Results indicate that the maximum principal stress occurred in the tensile surface region of the ceramic disk enclosed by the loading ball, with the highest rate at the middle and decreasing steadily as the radius of the disk radius increases (Figure 11). The FE stress analysis and close agreement between experimental and modeling results further validate that the theoretical model used in this study is appropriate for the ball-on-ring fixture. In conclusion, due to the advantages of this ball-on-ring test method, it would be advantageous to use it in obtaining large volumes of fracture strength data of engineered ceramics.

Acknowledgments

This project was partially supported through Oak Ridge National Laboratory and the Advanced Fuels Campaign (AFC) funding as well as an Integrated University Program (IUP) Graduate Fellowship.

ORCID

Adrianna E. Lupercio https://orcid.org/0000-0002-8974-3008
Ehsan Moshkelgosha https://orcid.org/0000-0001-7070-2428

REFERENCES

1. ASTM C1161-13, standard test method for flexural strength of advanced ceramics at ambient temperature. ASTM International. 2013.
2. Danzer R, Supancic P, Harrer W, Lube T, Borger A. Biaxial strength testing on mini specimens. In: Gdoutos EE, editor. Fracture of Nano and Engineering Materials and Structures. Dordrecht: Springer, 2006. https://doi.org/10.1007/1-4020-4972-2_292
3. Danzer R. Some notes on the correlation between fracture and defect statistics: are weibull statistics valid for very small specimens? J Eur Ceramic Soc. 2006;26(15):3043–9.
4. Ban S, Anusavice KJ. Influence of test method on failure stress of brittle dental materials. J Dent Res. 1990;69(12):1791–9.
5. Poolthong S, Mori T, Swain M. A comparison of the mechanical properties of three glass_ionemer cements. Dent Mater. 1994;13(2):220–7.
6. Shetty DK, Rosenfield AR, McGuire P, Bansal GK, Duckworth WH. Biaxial flexure tests for ceramics. Ceramic Bulletin. 1980;59(12):36–42.
7. Glandus J. Meaning of the biaxial flexure tests of discs for strength measurements. J Phys Coll. 1986;47:595–600.
8. Danzer R, Lube T, Supancic P, Damani R. Fracture of ceramics. Adv Eng Mater. 2008;10(4):275–98.
9. Torres Y, Bermejo R, Gotor FJ, Chicardi E, Llanes L. Analysis on the mechanical strength of WC-Co cemented carbides under uniaxial and biaxial bending. Mater Design. 2014;55:851–6.
10. Curkovic L, Bakic A, Kodvanj J, Haramina T. Flexural strength of alumina ceramics: Weibull analysis. Transaction of Famena. 2010.
11. Rinne H. Related Distributions from: The Weibull Distribution. A Handbook: CRC Press; 2008.
12. Savinykh AS, Mandel K, Razorenov SV, Kruger L. The influence of the cobalt content on the strength properties of tungsten carbide ceramics under dynamic load. Tech Phys. 2017;63(3):357–62.
13. Cousland GP, Cui XY, Smith AE, Stampfl APJ, Stampfl CM. Mechanical properties of zirconia, doped and undoped yttria-stabilized cubic zirconia from first-principles. J Phy Chem Solids. 2018;122:51–71.
14. Łatka L, Chicot D, Cattini A, Pawłowski L, Ambroziak A. Modeling of elastic modulus and hardness determination by indentation of porous yttria stabilized zirconia coatings. Surf Coat Technol. 2013;220:131–9.
15. Menvie Bekale V, Sattonnay G, Legros C, Huntz AM, Poissonnet S, Thomé L. Mechanical properties of cubic zirconia irradiated with swift heavy ions. J Nucl Mater. 2009;384(1):70–6.
16. Borik MA, Bublik VT, Kulebyakin AV, Lomonova EE, Milovich FO, Myzina VA, et al. Phase composition, structure and mechanical properties of PSZ (partially stabilized zirconia) crystals as a function of stabilizing impurity content. J Alloys Compd. 2014;586:S231–S5.
17. Ingel RP, Lewis D. Lattice parameters and density for Y2O3-stabilized ZrO2. J Am Ceramic Soc. 1986;69(4):325–35.
18. Auerkari P. Mechanical and physical properties of engineering alumina ceramics. VTT Manufacturing Technology. 1996.
19. Wereszczak A, Swab J, Kraft R. Effects of Machining on the Uniaxial and Equibiaxial Flexure Strength of CAP3 AD-995 Al2O3. Army Research Laboratory. 2005.
20. Wei W-CJ, Lin Y-P. Mechanical and thermal shock properties of size graded MgO–PSZ Refractory. J Eur Ceramic Soc. 2000;20(8):1159–67.
21. Carrasco-Pena A, Jordan R, Dieguez J, Cotonado-Rodriguez A, Ozdemir VB, Kwok K, et al. Design and development of ring-on-ring jig for biaxial strength testing of brittle ceramic composite materials: ZrB2-30wt% -SiB6. Adv Appl Ceram. 2019;118(4):159–68.
22. Chen Y-M, Smales RJ, Yip KH-K, Sung W-J. Translucency and biaxial flexural strength of four ceramic core materials. Dent Mater. 2008;24:1506–11.
23. Seidel J, Claussen N, Rodel J. Reliability of alumina ceramics: effect of grain size. J Eur Ceram Soc. 1995, 15, 395–404.

24. Reckziegel A. Properties and applications of high-performance ceramics made of zirconia. Aliaxis Utilities and Industry. 2015.
25. Kubota Y, Ashizuka M, Ishida E, Mitamura T. Influence of temperature on elastic modulus and strength of MgO-partially stabilized zirconia (Mg-PSZ). J Ceram Soc Japan. 1994;102(8):708–12.
26. Kim B, Jeon S, Tyne CJV, Park H, Lee H. Inter-granular phase formation and flexural strength of MgO partially stabilized zirconia by Al2O3 additions. J Ceram Process Res. 2016;17(5):459–63.
27. Jiang L, Guo S, Bian Y, Zhang M, Ding W. Effect of sintering temperature on mechanical properties of magnesia partially stabilized zirconia refractory. Ceram Int. 2016, 42, 10593–8.
28. Cheng M, Chen W, Sridhar KR. Experimental method for a dynamic biaxial flexural strength test of thin ceramic substrates. J Am Ceram Soc. 2002, 85(5), 1203–9.
29. Yilmaz H, Aydin C, Gul BE. Flexural strength and fracture toughness of dental core ceramics. J Prosthet Dent. 2007;98:120–8.
30. Stawarczyk B, Ozcan M, Hallmann L, Enger A, Mehl A, Hammerlet C. The effect of zirconia sitnering temperature on flexural strength, grain size, and contrast ratio. Clin Oral Invest. 2012;17:269–74.
31. Kosmač T, Oblak C, Jevnikar P, Funduk N, Marion L. The effect of surface grinding and sandblasting on flexural strength and reliability of Y-TZP zirconia ceramic. Dent Mater. 1999;15(6):426–33.
32. ReliaSoft: Weibull++. Hottinger Bruel & Kjaer Inc, Tucson, AZ. 2021.
33. Borger A, Supancic P, Danzer R. The ball on three balls test for strength testing of brittle discs: stress distribution in the disc. J Eur Ceram Soc. 2001;22:1425–36.
34. Silva PC, Moreira LP, Alves MFRP, Campos LQB, Simba BG, Santos Cd. Experimental analysis and finite element modeling of the piston-on-three balls testing of Y-TZP. Ceramica. 2020;66:30–42.
35. Moshkelgosha E, Mamivand M. Anisotropic Phase-Field Modeling of Crack Growth in Shape Memory Ceramics-Application to Zirconia. Proceedings of the ASME 2019. 2019.
36. Moshkelgosha E, Mamivand M. Phase field modeling of crack propagation in shape memory ceramics – Application to zirconia. Computat Mater Sci. 2020;174:109509.
37. Moshkelgosha E, Mamivand M. Concurrent modeling of martensitic transformation and crack growth in polycrystalline shape memory ceramics. Eng Fract Mech. 2021;241:107403.
38. Carlucci E, Tognarelli L. Mixed Weibull distribution as best representative of forced outage distribution to be implemented in blockism. ASME Power Conference. 2014.
39. Jiang S, Kececioglu D. Graphical representation of two mixed-Weibull distributions. IEEE Trans Reliab. 1992;41(2):241–7.
40. Karakoca A, Erisoglu U, Erisoglu M. A Comparison of the parameter estimation methods for biomodal mixture Weibull distribution with complete data. J Appl Stat. 2015;42(7):1472–89.
41. Gyekenyesi JP, Nemeth NN. Surface flaw reliability analysis of ceramic components with the SCARE finite element postprocessor program. 32nd International Gas and Turbine Conference and Exhibit. 1987.
42. Quinn GD. NIST Recommended Practice Guide Fractography of Ceramics and Glasses. National Institute of Standards and Technology. 2016.
43. Rice R. Ceramic Fracture Mode-Intergranular vs Transgranular Fracture. United States: Alfred conference on fractography of glasses and ceramics; 1996.

How to cite this article: Lupercio AE, Moshkelgosha E, Winters RC, et al. Ball-on-ring test validation for equibiaxial flexural strength testing of engineered ceramics. *Int J Ceramic Eng Sci*. 2021;3:128–139. https://doi.org/10.1002/ces2.10085